Soot and NO formation in counterflow ethylene/oxygen/nitrogen diffusion flames

Guo, Hongsheng; Liu, Fengshan; Smallwood, Gregory

Publisher's version / Version de l'éditeur:
https://doi.org/10.1088/1364-7830/8/3/003
Combustion Theory and Modelling, 8, September 3, pp. 475-489, 2004

INSTITUTE OF PHYSICS PUBLISHING COMBUSTION THEORY AND MODELLING

Combust. Theory Modelling **8** (2004) 475–489 PII: S1364-7830(04)70511-2

Soot and NO formation in counterflow ethylene/oxygen/nitrogen diffusion flames

Hongsheng Guo[1], **Fengshan Liu and Gregory J Smallwood**

Combustion Research Group, Institute for Chemical Process and Environmental Technology, National Research Council Canada, 1200 Montreal Road, Ottawa, Ontario, K1A 0R6, Canada

E-mail: hongsheng.guo@nrc-cnrc.gc.ca

Received 15 October 2003, in final form 26 March 2004
Published 4 May 2004
Online at stacks.iop.org/CTM/8/475
DOI: 10.1088/1364-7830/8/3/003

Abstract
Formation of soot and NO in counterflow ethylene/oxygen/nitrogen diffusion flames was numerically investigated. Detailed chemistry and complex thermal and transport properties were used. A simplified two-equation soot model was adopted. The results indicate that NO emission has negligible influence on soot formation. However, soot formation affects the emission of NO through the radiation induced thermal effect and the reaction induced chemical effect. When the oxygen index of the oxidant stream is lower, the relative influence of chemical reaction caused by soot on NO emission is more important, while the relative influence of the radiation induced thermal effect becomes more important for the flame with a higher oxygen index in the oxidant stream.

1. Introduction

Soot and NO_x are two typical pollutants emitted during the combustion of a hydrocarbon fuel. Understanding the mechanisms of soot and NO_x formation in combustion processes is of great interest to combustion scientists and engineers due to the need to control pollutant production. Many researchers have studied the formation mechanism of NO_x [1–3]. Proposed mechanisms for soot formation and oxidation in premixed and non-premixed flames have also been reported in many articles, such as [4–7].

Relatively little attention has been paid to the interaction between NO_x and soot formation. Turns *et al* [8, 9] and Wang and Niioka [10, 11] studied the influence of flame radiation on NO_x emission in turbulent jet flames and counterflow flames, and showed that the radiative heat transfer has a strong effect on NO_x emission in some flames. Liu *et al* [12] indicated that soot plays an important role in the radiation level in an axisymmetrical co-flow ethylene/air diffusion flame. Therefore, soot may affect NO_x formation via radiation. Atreya *et al* [13] investigated the relation between NO formation and radicals in counterflow diffusion flames and argued that soot/soot-precursor oxidation significantly reduced OH and O concentrations in the

[1] Author to whom any correspondence should be addressed.

primary reaction zone and contributed to the reduction of thermal NO formation. However, soot was not included in their numerical model. Radiative heat loss and NO_x emission of turbulent jet flames with preheated air were experimentally investigated by Fujimori *et al* [14]. They indicated that for an ethylene flame, as air temperature was increased, NO_x emission did not increase because of the radiative heat loss and competing oxidation of carbon or CO and nitrogen. Naik and Laurendeau [15] experimentally and numerically investigated NO emission in counterflow diffusion flames under sooting oxy-fuel high-temperature conditions, and showed that the agreement between predicted and measured NO concentration is poorer. They argued that it is because the enhanced radiative heat loss caused by soot was not included in the numerical model. To our knowledge, no detailed numerical study on the interaction of soot and NO_x has been reported by including both soot and NO_x in the model.

In this paper, we investigate soot and NO, the dominant component of NO_x, formation in counterflow ethylene/oxygen/nitrogen diffusion flames by numerical simulation. The objective is to use the details from the numerical simulation to gain further insight into the mechanisms of soot and NO formation, with emphasis on the interaction of soot and NO processes. A detailed chemical reaction scheme for the gaseous phase and a simplified two-equation soot model were used.

2. Numerical model

2.1. Gaseous phase governing equations

The flame configuration studied in this paper is a counterflow, axisymmetric laminar diffusion flame. By assuming the stagnation point flow approximation [16], the governing equations for the gaseous phase are written as

$$\frac{\mathrm{d}\rho}{\mathrm{d}t} + \frac{\mathrm{d}V}{\mathrm{d}x} = -2\rho G \tag{1}$$

$$L(G) = \frac{\mathrm{d}}{\mathrm{d}x}\left(\mu\frac{\mathrm{d}G}{\mathrm{d}x}\right) - \rho G^2 + \rho\left(\frac{\mathrm{d}a}{\mathrm{d}t} + a^2\right) \tag{2}$$

$$C_p L(T) = \frac{\mathrm{d}}{\mathrm{d}x}\left(\lambda\frac{\mathrm{d}T}{\mathrm{d}x}\right) - \sum_{k=1}^{KK+1}\rho Y_k V_k C_{pk}\frac{\mathrm{d}T}{\mathrm{d}x} - \sum_{k=1}^{KK+1} h_k\omega_k M_k + q_\mathrm{r} \tag{3}$$

$$L(Y_k) = -\frac{\mathrm{d}}{\mathrm{d}x}(\rho Y_k V_k) + \omega_k M_k \tag{4}$$

where

$$L(\phi) = \frac{\mathrm{d}\phi}{\mathrm{d}t} + V\left(\frac{\mathrm{d}\phi}{\mathrm{d}x}\right).$$

t is the time, x the axial coordinate, V the axial mass flow rate and a is the stretch rate. The quantity G is a combined function of the stretch rate and the stream function, ρ is the density of the mixture, T the temperature, Y_k the mass fraction of the kth gas species, μ the viscosity of the mixture, C_{pk} the constant pressure heat capacity of the kth gas species, M_k the molecular weight of the kth gas species, h_k, V_k and ω_k are, respectively, the species enthalpy, the diffusion velocity and the molar production rate of the kth gas species and KK is the total gas species number. The production rates of gas species include the contribution due to the soot inception, surface growth and oxidation (see below). The quantities with subscript $KK + 1$ correspond to those of soot. As an approximation, the thermal properties of graphite, obtained from JANAF thermochemical tables [17], were used to represent those of soot.

The last term on the right-hand side of equation (3), q_r, is the radiation heat loss. The effects of gas and soot radiation on soot formation in counterflow ethylene diffusion flames have been investigated in [18] by comparing the results from three different radiation models: the adiabatic, an optically thin model and the discrete ordinates method coupled to an accurate band model. It is indicated that the radiation reabsorption has an insignificant effect on temperature and soot formation in counterflow ethylene/oxygen/nitrogen diffusion flames. The difference between the results from the simulations with the optically thin model and the discrete ordinates method is negligible. For the sake of simplification, the radiation heat loss due to CO_2, H_2O, CO and soot was calculated by the following optically thin model in this study:

$$q_r = -4\sigma K_p(T^4 - T_\infty^4) - Cf_v T^5 \tag{5}$$

$$K_p = p\sum x_i K_{pi} \tag{6}$$

where σ is the Stefan–Boltzmann constant and K_p is the Planck mean absorption coefficient of the mixture. T_∞ and P, respectively, denote the environmental temperature (300 K was used in this paper) and pressure. K_{pi} and x_i are the Planck mean absorption coefficient and mole fraction of the ith emitting gas species (which is CO_2, H_2O or CO). The Planck mean absorption coefficients of the emitting gas species were obtained by fitting the data given by Tien [19]. The quantity f_v is the soot volume fraction and C is a constant equal to 3.334E−10 (giving a power density in watts cc^{-1} for T in Kelvin) [20].

The diffusion velocity (V_k) is written as

$$V_k = -\frac{1}{Y_k} D_k \frac{\partial Y_k}{\partial x} + V_{Tk} + V_c \qquad k = 1, 2, \ldots, KK \tag{7}$$

where V_{Tk} is the thermal diffusion velocity for the kth gas species. In this paper, only the thermal diffusion velocities of H_2 and H were considered by the method given in [21], while those of all other species were set as zero. The correction diffusion velocity V_c was used to ensure that the net diffusive flux of all gas species and soot is zero [21]. The quantity D_k was related to the binary diffusion coefficients through the relation

$$D_k = \frac{1 - X_k}{\sum_{j\neq k}^{KK} X_j / D_{jk}} \qquad k = 1, 2, \ldots, KK \tag{8}$$

where X_k is the mole fraction of the kth species and D_{jk} is the binary diffusion coefficient.

2.2. Soot model

Modelling of soot formation can be carried out by a detailed kinetic model, a purely empirical model or a semi-empirical model. Detailed soot kinetic models, such as those by Frenklach *et al* [5, 22, 23], are currently highly complex and computationally expensive. Conversely, the applicability of purely empirical soot models is questionable under conditions different from those under which they were originally formulated. Based on some semi-empirical assumptions, the model developed by Leung *et al* [24] and Fairwhether *et al* [25] has been successfully used in our previous studies [7, 26] for the simulations of two-dimensional ethylene/air diffusion flames. This soot model was also used in this paper.

Two transport equations were solved for soot mass fraction and number density, respectively. They are

$$V\frac{\partial Y_s}{\partial x} = -\frac{\partial}{\partial x}(\rho V_{T,s} Y_s) + S_m \tag{9}$$

$$V\frac{\partial N}{\partial x} = -\frac{\partial}{\partial x}(\rho V_{T,s} N) + S_N \tag{10}$$

where Y_s is the soot mass fraction and N is the soot number density, defined as the particle number per unit mass of mixture. The quantity $V_{T,s}$ is the particle thermophoretic velocity. It was obtained by the expression [27]:

$$V_{T,s} = -0.54\frac{\mu}{\rho T}\frac{\partial T}{\partial x}. \tag{11}$$

The source term S_m in equation (9) accounts for the contributions of soot nucleation (ω_n), surface growth (ω_g) and oxidation (ω_O). Therefore,

$$S_m = \omega_n + \omega_g - \omega_O. \tag{12}$$

The acetylene based semi-empirical soot model developed by Leung *et al* [24] and Fairwhether *et al* [25] was used to obtain the first two terms on the right-hand side of equation (12). The model assumes the chemical reactions for nucleation and surface growth, respectively, as

$$C_2H_2 \rightarrow 2C(S) + H_2 \tag{R1}$$

$$C_2H_2 + nC(S) \rightarrow (n+2)C(S) + H_2 \tag{R2}$$

with the reaction rates given by the expressions

$$r_1 = k_1(T)[C_2H_2] \tag{13}$$

$$r_2 = k_2(T)f(A_s)[C_2H_2] \tag{14}$$

where $f(A_s)$ denotes the functional dependence on soot surface area per unit volume. Similar to Fairwhether *et al* [25] and our previous studies [7, 26], a simple linear functional dependence was used, i.e. $f(A_s) = A_s$. While the rate constants $k_1(T)$ and $k_2(T)$ were basically taken from Leung *et al* [24], a small adjustment was made for $k_2(T)$ to fit the measured soot volume fractions by Hwang and Chung [28] for the studied flames.

Soot oxidation occurs primarily as a result of attack by molecular oxygen and the OH radical. The O radical also contributes to soot oxidation in some regions. Therefore, the soot oxidation by O_2, OH and O were accounted for by the following reactions in this paper:

$$0.5O_2 + C(S) \rightarrow CO \tag{R3}$$

$$OH + C(S) \rightarrow CO + H \tag{R4}$$

$$O + C(S) \rightarrow CO. \tag{R5}$$

The reaction rates for these three reactions were obtained as

$$r_3 = k_3(T)T^{1/2}A_s[O_2] \tag{15}$$

$$r_4 = \varphi_{OH}k_4(T)T^{-1/2}A_sX_{OH} \tag{16}$$

$$r_5 = \varphi_O k_5(T)T^{-1/2}A_sX_O \tag{17}$$

where X_{OH} and X_O denote the mole fractions of OH and O, and φ_{OH} and φ_O are the collision efficiencies for OH and O attack on soot particles. A collision efficiency of 0.13 [29] was used for OH, and 0.5 [30] for O attack on soot particles.

All the reaction rate constants, k_i ($i = 1, \ldots, 5$), are summarized in table 1.

The source term S_N in equation (10) accounts for the soot nucleation and agglomeration, and was calculated as [24, 25]:

$$S_N = \frac{2}{C_{min}}N_A r_1 - 2C_a\left(\frac{6M_{C(S)}}{\pi\rho_{C(S)}}\right)^{1/6}\left(\frac{6\kappa T}{\rho_{C(S)}}\right)^{1/2}[C(S)]^{1/6}[\rho N]^{11/6} \tag{18}$$

Table 1. Rate constants, as $k_i(T) = A\exp(-E/RT)$ (units are kg, m, s, kmol and K).

k_i	A	E	Reference
k_1	10 000.0	41.0	[24]
k_2	3 468.0	24.0	—
k_3	10 000.0	39.0	[24]
k_4	106.0	0.0	[29]
k_5	55.4	0.0	[30]

where N_A is Avogadro's number (6.022×10^{26} particles kmol^{-1}), C_{min} is the number of carbon atoms in the incipient carbon particle (100) [24], κ is the Boltzmann constant (1.38×10^{-23} J K^{-1}), $\rho_{C(S)}$ is the soot density (1900 kg m^{-3}), [C(S)] is the mole concentration of soot (kmol m^{-3}), $M_{C(S)}$ is the molar mass of soot (12.011 kg kmol^{-1}) and C_a is the agglomeration rate constant, for which a value of 9.0 [24] was used.

2.3. Numerical methods

The calculations were carried out with a code revised from that of Kee *et al* [31]. Upwind and centre difference schemes were, respectively, used for the convective and diffusion terms in all the governing equations. Adaptive refinement of meshes was done. The pressure and environment temperature were, respectively, 1 atm and 300 K. The distance between the two opposed nozzles was 1.5 cm for all the calculations.

The chemical reaction mechanism adopted is essentially from GRI-Mech 3.0 [32]. The thermal and transport properties were obtained by using the database of GRI-Mech 3.0 and the algorithms given in [21, 33].

3. Results and discussion

Three flames investigated experimentally by Hwang and Chung [28] were simulated. The fuel stream is pure ethylene for all the three flames, while the oxidant streams are different mixtures of nitrogen and oxygen. The mole fractions of oxygen, called oxygen index (X_{O_2}), of the oxidant stream for the three flames are, respectively, 20%, 24% and 28%. The stretch rate is 27.5 1/s. This stretch rate was selected to match the global axial velocity gradient in the experiments [28].

The calculations were first carried out by two reaction schemes: the full GRI-Mech 3.0 [32] and its revised version obtained by simply removing all the reactions and species related to NO_x formation from the full GRI-Mech 3.0 scheme.

The soot volume fraction profiles obtained by the two reaction schemes for the three flames were compared. It was found that there is almost no discernable difference in the predicted soot volume fraction profiles between the results obtained by the two reaction schemes. Accordingly, we conclude that the formation of NO_x has little effect on the production and oxidation of soot in these flames. Therefore, we concentrate on the influence of soot on NO emission in this paper. Hereafter, all the results presented were obtained by the full GRI-Mech 3.0 reaction scheme.

The predicted soot volume fractions are compared with those measured by Hwang and Chung [28] in figure 1. To clearly show the relative positions of soot, peak flame temperature and peak NO concentration in all figures for the three flame conditions, the data have been aligned such that the stagnation planes of both experiment and simulations are at $X = 0.0$ cm in all the plots, i.e. $X = x - x_s$ with x_s being the stagnation plane position. The fuel stream comes

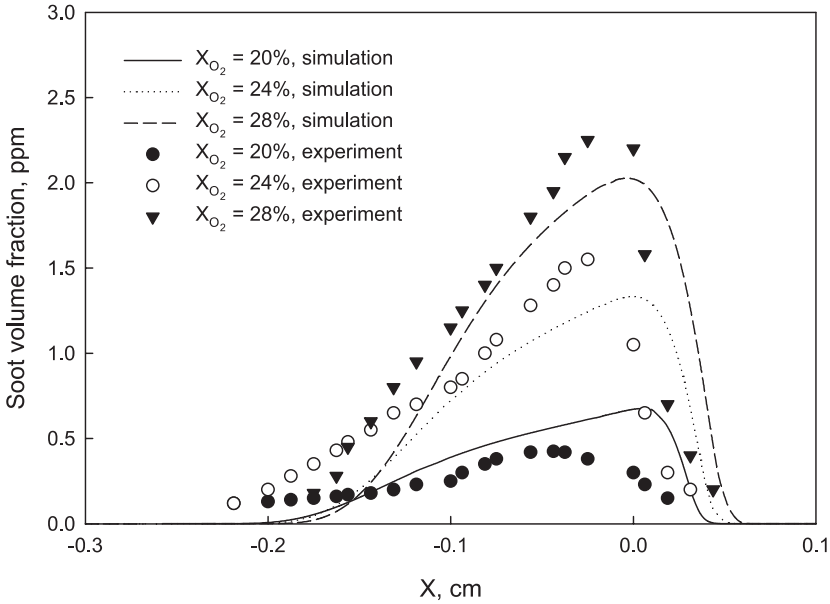

Figure 1. Soot volume fractions obtained from the current simulations and the experiment [28].

from the right-hand side, and the oxidant stream from the left. It is observed that there are some differences between the simulation and experiment. The peak soot volume fractions of the flames with oxygen indices of 24% and 28% are a little underpredicted, and the positions of peak soot volume fraction predicted are slightly shifted to the fuel side. However, the simulation captured the general soot characteristics in these flames. The soot volume fraction increases when the oxygen index is raised. The predicted peak soot volume fraction of the flame with the oxygen index of 20% is 0.68 ppm, while this value is increased to 2.03 ppm for the flame with the oxygen index of 28%. Therefore, the soot model used is basically reasonable.

Figure 2 illustrates the predicted rates of the soot inception, surface growth and oxidation for the flame with the oxygen index of 28%. It is observed that the inception rate is much smaller than the surface growth rate, and thus the surface growth dominates the soot mass growth. This is consistent with the current understanding of the soot formation mechanism. For soot oxidation, the radical OH is the most significant species in terms of oxidizing the soot particles. Comparing the soot formation (the sum of inception and surface growth) and oxidation rates, it is found that the oxidation rate is one order of magnitude smaller than the formation rate. Therefore, the oxidation process is negligible in this flame. This is because the flame is located on the oxidizer side of the stagnation plane ($X = 0.0$), such that soot particles once incepted are transported away from the flame towards the stagnation plane. These kinds of flames were classified as soot formation (SF) flames in [28]. The results for the other two flame conditions are similar.

Soot may affect NO emission through the variations of the radiation induced temperature and the reaction induced radical concentrations, i.e. effects of thermal and chemical reactions. With the former, the existence of soot causes a flame temperature reduction due to radiation heat loss, whereas the latter results from the competition for some species by both soot and NO formation. To investigate these effects, three simulations were conducted for every flame. The first simulation (SIM1, indicated as *With soot* in all the plots) was conducted by including

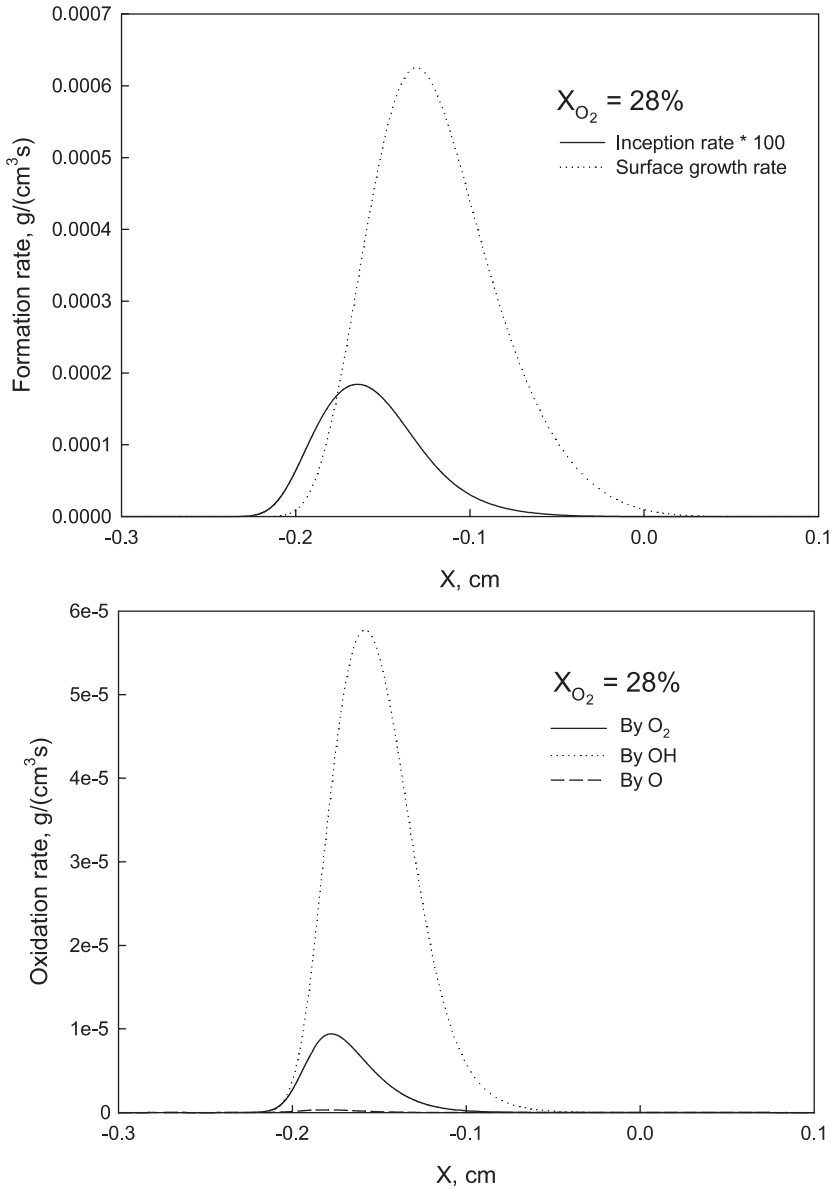

Figure 2. Rates of soot inception, surface growth and oxidation of the flame with oxygen index of 28%.

both NO_x and soot in the model, while the inception and surface growth rates of soot were set as zero in the second (SIM2, indicated as *Without soot*, *fixed T* in all the plots) and third (SIM3, indicated as *Without soot* in all the plots) simulations for every flame. The temperatures of the second simulation for all the flames were kept the same as those in the first simulation, whereas the temperatures were calculated in the third simulation. Therefore, the difference in results between the first and second simulations is caused by the chemical reaction effect of soot, while the difference between the second and third simulations is mainly caused by the radiation induced thermal (temperature) effect.

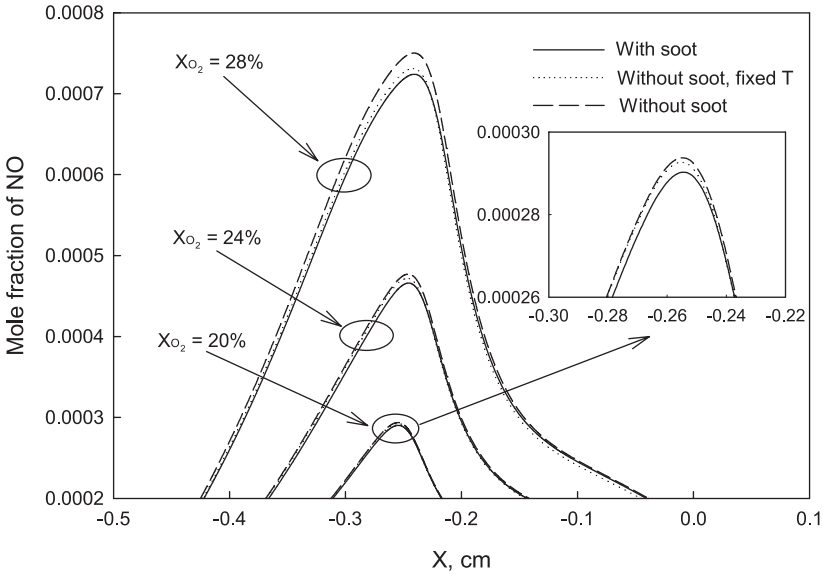

Figure 3. NO profiles of the three flames.

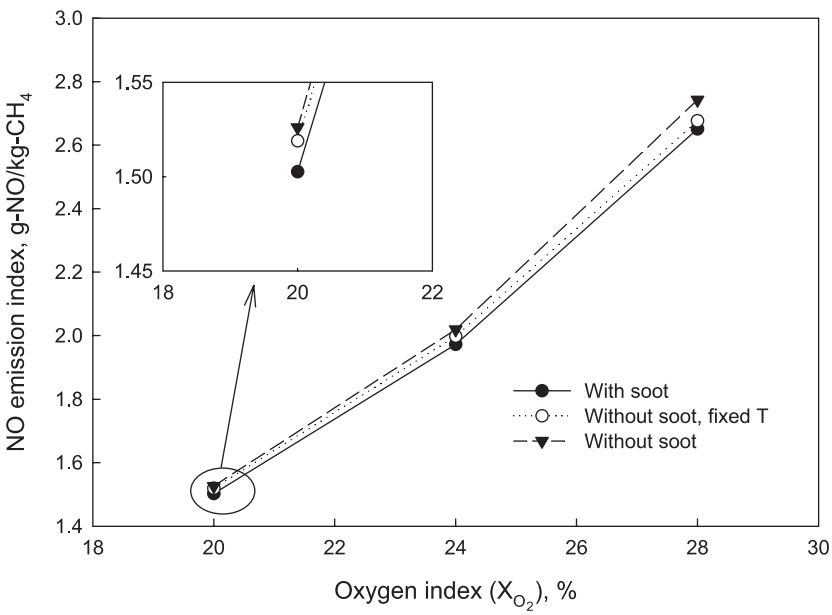

Figure 4. The emission index of NO.

Figure 3 depicts the predicted profiles of NO concentration in the three flames. The predicted emission index of NO, defined as the production of NO per unit mass of fuel (C_2H_4) consumption (g-NO/kg-C_2H_4), is shown in figure 4. It is observed that soot does affect NO emission. The formation of soot in a flame suppresses NO emission. The influence is enhanced when the oxygen index in the oxidant stream is increased. When the oxygen index in the oxidant stream is 20%, the difference in the peak NO concentration between the simulations with soot

included (SIM1) and without soot (SIM3) is only about 4 ppm. This difference is increased to 26 ppm for the flame with the oxygen index of 28% in the oxidant stream. Apparently, this is because soot volume fraction in flame increases when the oxygen index is raised (figure 1), leading to greater radiation heat loss and stronger competition for some radicals by both soot and NO formation.

Moreover, it is noted from figures 3 and 4 that when the oxygen index is 20%, the influence of soot on NO formation is mainly through the chemical reaction. However, with the increase of the oxygen index in the oxidant stream, the radiation induced thermal effect increases. For the flame with the oxygen index of 28%, the thermal effect becomes more significant than the chemical effect. The variation of the relative effects of thermal and chemical reaction of soot on NO formation is caused by the disparity in the soot volume fraction and the relative contribution of thermal and prompt routes to the total NO production in the flames, when the oxygen index of the oxidant stream changes. Detailed discussions on the influences of thermal and chemical reaction of soot on NO formation will be given in the following paragraphs.

It is well known that NO is formed mainly by thermal and prompt routes. The thermal route comprises the three reactions: $N + NO = N_2 + O$, $N + O_2 = NO + O$ and $N + OH = NO + H$. The first one is the initiation reaction that converts molecular nitrogen to atomic nitrogen and NO. The prompt NO is formed primarily by a reaction sequence that is initiated by the rapid reaction of hydrocarbon radicals with molecular nitrogen [1]. Among these prompt initiation reactions, the most significant one is: $CH+N_2 = HCN+N$. The HCN produced by this reaction (and other prompt initiation reactions) is converted rapidly to NO mainly through the path: $HCN \rightarrow NCO \rightarrow NH \rightarrow N \rightarrow NO$ [1, 3]. The initiation reaction $CH + N_2 = HCN + N$ is the rate-limiting step for this process. The last step of this process (from N to NO) is through the reaction $N + OH = NO + H$, being the same as the last reaction of the thermal route. Therefore, the temperature and the concentrations of CH, O and OH are the most important factors affecting NO formation. In the following paragraphs, the variations of these factors caused by soot will be checked and discussed to analyse the effect of soot on NO formation.

We first analyse the flame with the oxygen index of 20%. The prompt route dominates the NO formation in this flame. This can be shown by the rate profiles of the two reactions: $N + NO = N_2 + O$ and $CH + N_2 = HCN + N$ in figure 5(*a*), where the negative rate means molecular nitrogen is consumed. As discussed, the former reaction is the initial reaction of the thermal NO formation route, and the latter is the most important initial reaction of the prompt route for NO formation. It is noted that while the prompt route initiates NO formation in the flame zone, the reaction $N + NO = N_2 + O$ forms NO near the oxidant side (left) and converts atomic nitrogen and NO back to molecular nitrogen in the flame zone. These two reactions are strongly coupled with each other in the flame zone. The conversion of atomic nitrogen and NO back to molecular nitrogen by the reaction $N + NO = N_2 + O$ in the flame zone is mainly due to the production of atomic nitrogen by the reaction $CH + N_2 = HCN + N$. Because of the higher rate of the reaction $CH + N_2 = HCN + N$, the absolute molecular nitrogen consumption rate in the flame zone is much higher than that near the oxidant side. Therefore, most NO in this flame is formed through the prompt route.

Figure 5(*a*) also indicates that the soot caused rate variation of the thermal NO initiation reaction $N + NO = N_2 + O$ in the flame with the oxygen index of 20% is negligible. This is because soot volume fraction in this flame is quite low (figure 1) and peaks in a region with lower temperature, only about 1100 K. Therefore, the variation of radiation induced temperature due to soot is very small (as shown in figure 6). Meanwhile the variation in the concentration of radical O due to soot is also very small (figure 7). Consequently, the effect of soot on the reaction $N + NO = N_2 + O$ can be neglected for this flame.

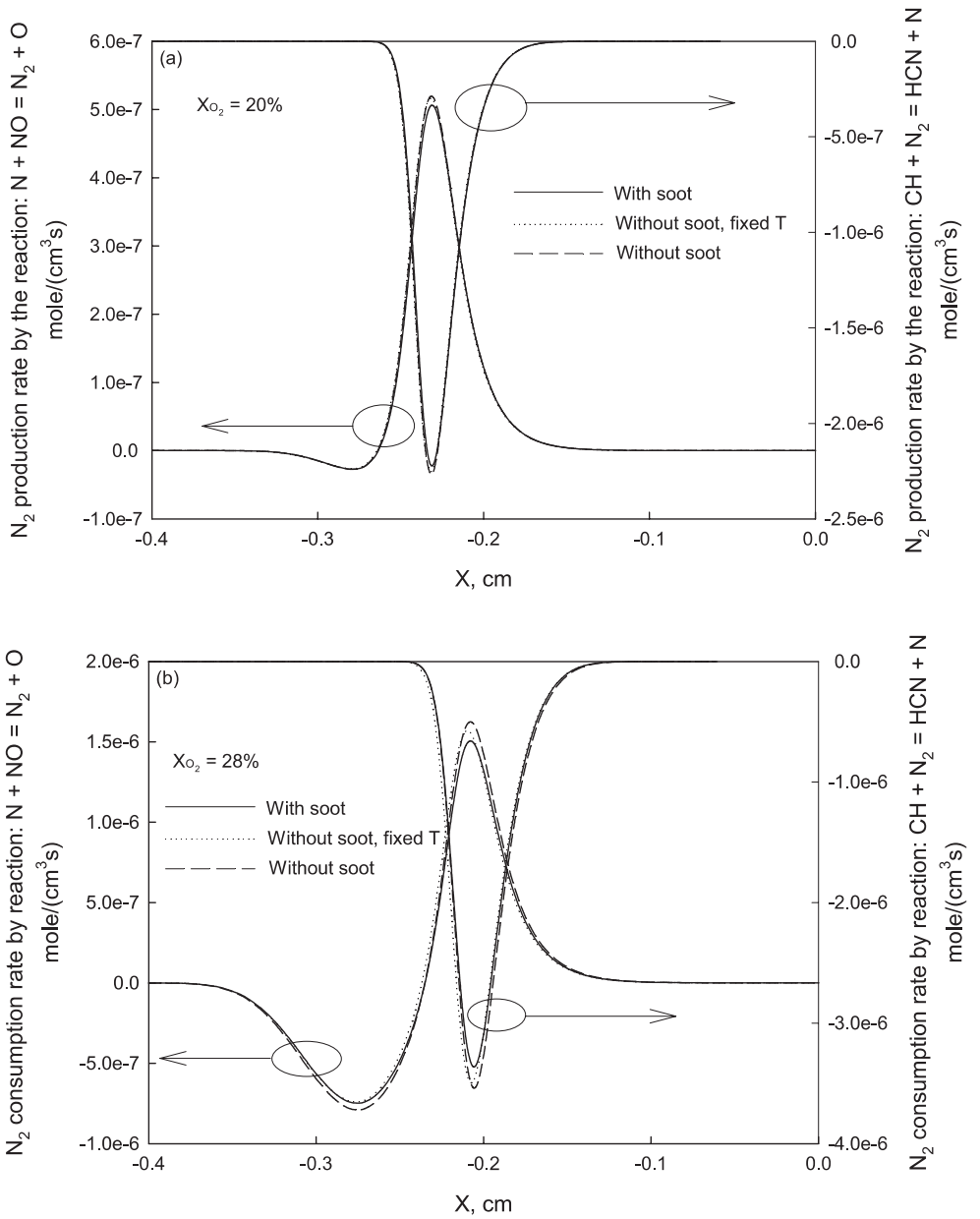

Figure 5. Reaction rate profiles of the reactions: N + NO = N_2 + O and CH + N_2 = HCN + N.

On the other hand, figure 8 shows that the formation of soot reduces the concentration of radical CH in the flame with oxygen index of 20%, in spite of the lower soot volume fraction. This reduction is mainly owing to the chemical reaction effect of soot. As the oxidation in the flames studied in this paper is negligible, the influence of soot on the concentration of CH primarily results from soot formation. A sensitivity analysis indicates that the dominant reaction for CH radical production is the reverse reaction of CH + H_2 = H + CH_2, while an important CH_2 production reaction is O + C_2H_2 = CO + CH_2. Acetylene (C_2H_2) is the

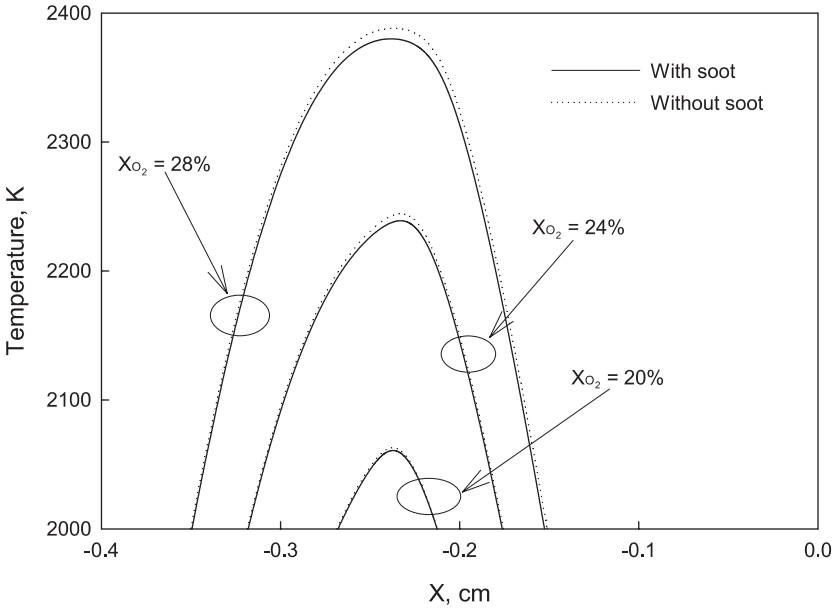

Figure 6. Temperature profiles of three flames.

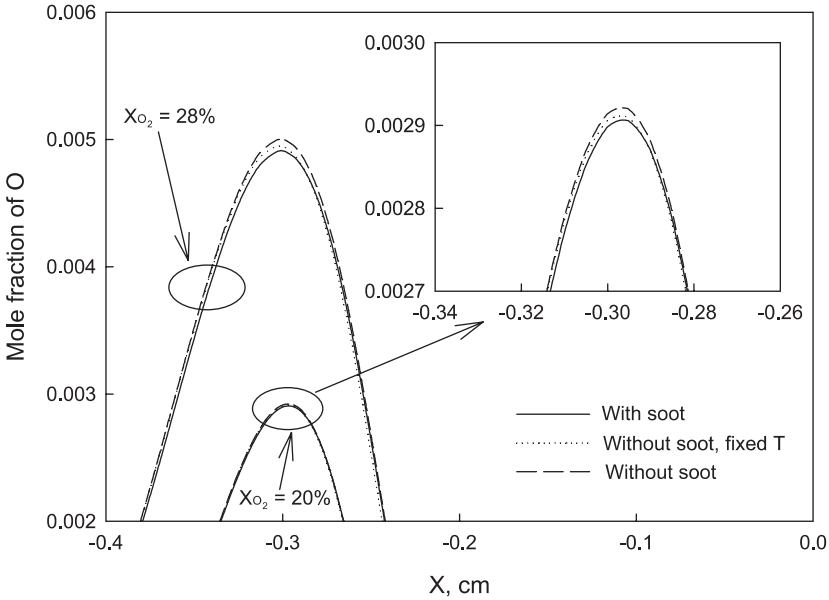

Figure 7. Mole fraction of radical O.

most important precursor of soot. Its consumption by soot inception and surface growth reduces the concentration of CH radical by these two reactions. As a result, the prompt route initial reaction, $CH + N_2 = HCN + N$, is affected by soot due to the variation in the concentration of CH (figure 5(*a*)). Although the produced atomic nitrogen and HCN by the reaction $CH+N_2 = HCN+N$ are partially converted back to molecular nitrogen by the reaction

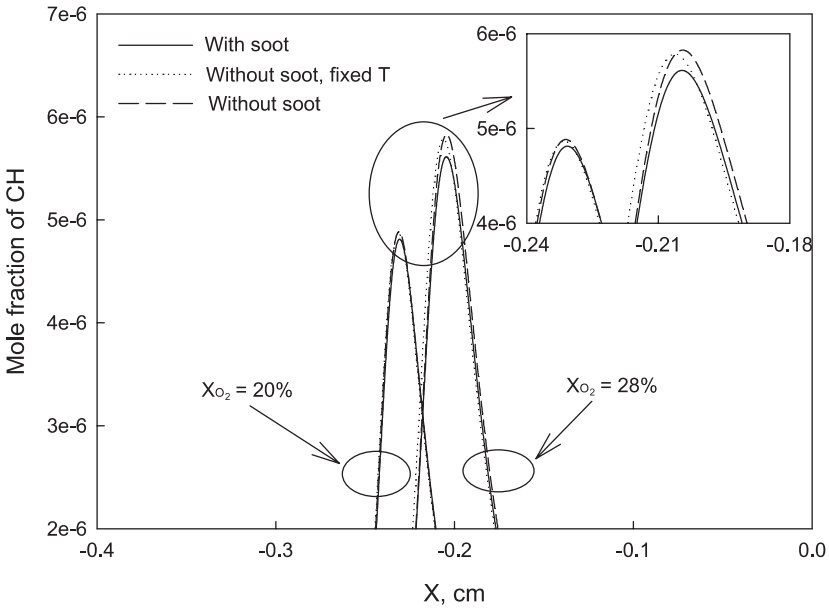

Figure 8. Profiles of radical CH mole fraction.

$N + NO = N_2 + O$ in the primary reaction zone, the simulation indicates that the peak rate variation of the latter due to the chemical effect of soot (the difference between SIM1 and SIM2) for this flame is only about $\frac{1}{3}$ as that of the former ($CH + N_2 = HCN + N$). Since the prompt route dominates the NO formation in the flame with oxygen index of 20%, the effect of soot on NO formation in this flame is mainly caused by the chemical reaction effect.

The variation of radical OH due to soot in the flame with the oxygen index of 20% is not significant either, as illustrated in figure 9. The influence of soot on NO emission through OH can also be neglected for this flame.

When the oxygen index increases to 28%, the flame temperature rises, as shown in figure 6. The contribution of the thermal route to the total NO production increases, as in figure 5(*b*). The soot volume fraction peaks in the region with temperature about 1300 K for this flame.

Because of the higher soot volume fraction peaking in a relatively higher temperature region in the flame with the oxygen index of 28%, the soot induced temperature variation also increases, compared to the flame with the oxygen index of 20% (figure 6). Meanwhile, soot causes the disparity in the concentration of the O radical (as shown in figure 7). This disparity is mainly caused by the thermal effect of soot in the region where molecular nitrogen is consumed by the reaction $N + NO = N_2 + O$ ($X > -0.3$). As a result, the soot caused molecular nitrogen consumption rate variation by the reaction $N + NO = N_2 + O$ is enhanced, compared to the flame with the oxygen index of 20% (figure 5). This enhancement is primarily owing to the thermal effect of soot. The simulations indicate that the peak nitrogen consumption rate by the reaction $N + NO = N_2 + O$ is increased by 5.5% for the flame with oxygen index of 28% because of the thermal effect of soot, while it is increased by only 1.0% for the flame with the oxygen index of 20%, when soot is neglected in the simulation.

The influence of soot on the concentration of OH is also enhanced in the flame with oxygen index of 28%. The variation due to the thermal effect of soot is larger than that due to the chemical reaction effect, as in figure 9. The chemical effect of soot actually increases the concentration of OH, when soot is taken into account. This is because of the decrease

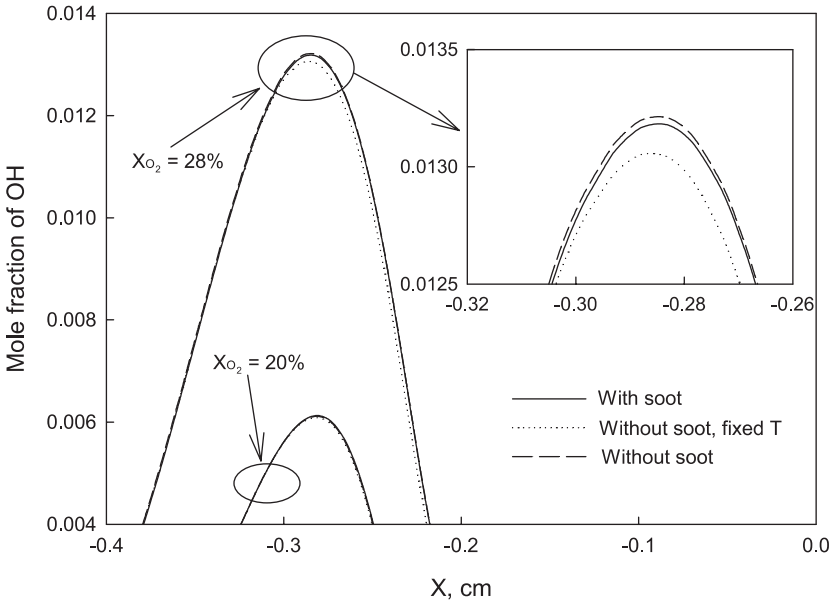

Figure 9. Mole fraction of radical OH.

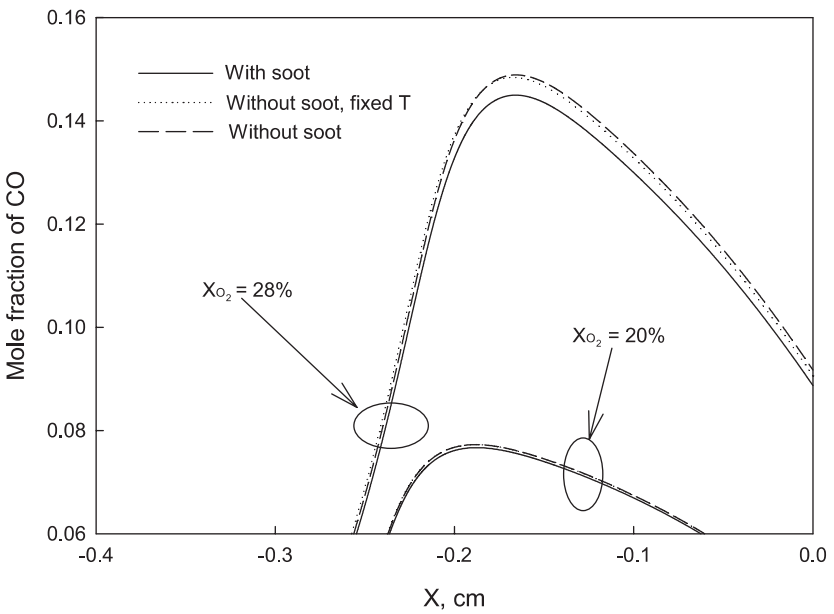

Figure 10. Mole fractions of CO.

in the concentration of CO (figure 10). As for CH_2, the reaction $O + C_2H_2 = CO + CH_2$ is also an important production reaction for CO. The inception and surface growth of soot consumes C_2H_2, and thus lowers the formation rate of CO in the flame. This causes less OH to be consumed by the reaction $CO + OH = H + CO_2$, when soot is taken into account in the simulation. Although oxidation of soot also affects the OH concentration, this influence is

tiny due to the negligible soot oxidation in the flames studied (as shown in figure 2). Being different from the chemical effect, the thermal effect of soot reduces the concentration of OH in the flame. Therefore, the formation of soot suppresses NO formation through the variation of OH concentration due to its thermal effect.

The higher soot volume fraction in the flame with the oxygen index of 28% also results in the variations in the concentration of CH and thus the rate of the reaction $CH + N_2 = HCN + N$ in the flame zone. The chemical effect of soot on this reaction is more significant than that of the thermal effect (as in figures 5(*b*) and 8). However, the nitrogen consumption region by the reaction $CH + N_2 = HCN + N$ is slightly less than that by the reaction $N + NO = N_2 + O$, and the atomic nitrogen formed by the reaction $CH + N_2 = HCN + N$ in the flame zone is partially converted back to molecular nitrogen by the reaction $N + NO = N_2 + O$. In addition, as indicated above, the suppression of soot on the concentration of OH is because of its thermal effect. Consequently, the thermal effect of soot on the formation of NO in the flame with the oxygen index of 28% is larger than the chemical effect.

From the above discussions, we conclude that soot process does moderately affect the formation of NO in counterflow ethylene diffusion flames. When the oxygen index in the oxidant stream is at atmospheric levels, this effect is mainly through chemical reaction, while the effect is mainly through thermal influence for flames with higher oxygen index in the oxidant stream.

Although the effect of soot on NO formation for the flames studied in this paper is not very strong, it may become significant for heavily sooting flames. It has been demonstrated that soot plays an important role in the radiation level in a two-dimensional axisymmetrical laminar ethylene diffusion flame [12]. As a result, we expect that the effect of soot on NO formation may be enhanced in this kind of flame. This issue will be investigated in the future.

Finally, we should point out that the flames studied in this paper are soot formation (SF) flames. The influence of soot oxidation on NO formation is negligible for these flames. However, for those soot formation/oxidation (SFO) [28] flames, the effect of soot oxidation on NO formation may not be negligible. This issue is also a topic of interest for the future.

4. Concluding remarks

Soot and NO formation in $C_2H_4/N_2/O_2$ diffusion flames have been numerically investigated. The results indicate that the process of NO formation has almost no effect on soot formation. However, soot does affect the formation of NO. The formation of soot in a flame suppresses NO emission.

Soot affects NO emission through the variations of radiation induced temperature and the reaction induced radical concentrations, i.e. effects of thermal and chemical reactions. The former is due to the existence of soot that causes the flame temperature variation, and the latter results from the competition for some species by both soot and NO formation. The most important competing species is acetylene (C_2H_2). When the oxygen index of the oxidant stream is lower, the relative influence of chemical reaction caused by soot on NO formation is more important, while the relative influence of radiation induced thermal effect becomes dominant for the flame with higher oxygen index in the oxidant stream. The variation of the relative influence of thermal and chemical reaction of soot is caused by the variation in the absolute soot volume fraction and the relative contribution of thermal and prompt routes to NO formation in the flame. For the lower oxygen index flame, the prompt route dominates the formation of NO in the flame, while the thermal route becomes significant for the higher oxygen index flame.

Acknowledgment

This paper was presented at the 19th International Colloquium on the Dynamics of Explosions and Reactive Systems, Hakone, Japan, July 2003.

References

[1] Miller J A and Bowman C T 1989 *Prog. Energy Combust. Sci.* **15** 287–338
[2] Nishioka M, Nakagawa S, Ishikawa Y and Takeno T 1994 *Combust. Flame* **98** 127–38
[3] Ju Y and Niioka T 1997 *Combust. Theory Modelling* **1** 243–58
[4] Kennedy I M 1997 *Prog. Energy Combust. Sci.* **23** 95–132
[5] Frenklach M and Wang H 1990 *Proc. Combust. Inst.* **23** 1559–66
[6] Xu F and Faeth M 2001 *Combust. Flame* **125** 804
[7] Guo H, Liu F, Smallwood G J and Gülder Ö L 2002 *Proc. Combust. Inst.* **29** 2359–65
[8] Turns S R and Myhr F H 1991 *Combust. Flame* **87** 319–35
[9] Turns S R, Myhr F H, Bandaru R V and Maund E R 1993 *Combust. Flame* **93** 255–69
[10] Wang J and Niioka T 2002 *Combust. Theory Modelling* **5** 385–98
[11] Wang J and Niioka T 2002 *Proc. Combust. Inst.* **29** 2211–18
[12] Liu F, Guo H, Smallwood G J and Gülder Ö L 2002 *J. Quant. Spectrosc. Radiat. Transfer* **73** 409–21
[13] Atreya A, Zhang C, Kim H K, Shamim T and Suh J 1996 *Proc. Combust. Inst.* **26** 2181–9
[14] Fujimori T, Hamano Y and Sato J 2000 *Proc. Combust. Inst.* **28** 455–61
[15] Naik S V and Laurendeau N M 2002 *Combust. Flame* **129** 112–19
[16] Giovangigli V and Smooke M D 1987 *Combust. Sci. Technol.* **53** 23–49
[17] Chase M W, Davies C A, Downey J R, Frurlp D J, McDonald R A and Syverud A N 1985 *JANAF Thermochemical Tables* 3rd edn (New York: American Chemical Society and American Institute of Physics)
[18] Liu F, Guo H, Smallwood G J and Hafi M E 2004 *J. Quant. Spectrosc. Radiat. Transfer* **84** 501–11
[19] Tien C L 1967 *Adv. Heat Transfer* **5** 253–324
[20] Smooke M D, Mcenally C S, Pfefferle L D, Hall R J and Colket M B 1999 *Combust. Flame* **117** 117–39
[21] Kee R J, Warnatz J and Miller J A 1983 *Sandia Report* SAND 83-8209
[22] Frenklach M, Clary D W, Gardiner W C and Stein S E 1984 *Combust. Inst.* **20** 887–901
[23] Frenklach M and Wang H 1994 *Soot Formation in Combustion: Mechanisms and Models* ed H Bockhorn (*Springer Series in Chemical Physics* vol 59) (Berlin: Springer) pp 164–90
[24] Leung K M, Lindstedt R P and Jones W P 1991 *Combust. Flame* **87** 289–305
[25] Fairwhether M, Jones W P and Lindstedt R P 1992 *Combust. Flame* **89** 45–63
[26] Guo H, Liu F, Smallwood G J and Gülder Ö L 2002 *Combust. Theory Modelling* **6** 173–87
[27] Talbot L, Cheng R K, Schefer R W M and Willis D R 1980 *J. Fluids Mech.* **101** 737–58
[28] Hwang J Y and Chung S H 2001 *Combust. Flame* **125** 752–67
[29] Neoh K G, Howard J B and Sarofim A F 1981 *Particulate Carbon: Formation During Combustion* ed D C Siegla and G W Smith (New York: Plenum) P.261–82
[30] Bradley D, Dixon-Lewis G, Habik S E and Mushi E M 1984 *Proc. Combust. Inst.* **20** 931–40
[31] Kee R J, Grcar J F, Smooke M D and Miller J A 1994 *Sandia Report* SAND85-8240
[32] Smith G P *et al* http://www.me.berkeley.edu/gri_mech/
[33] Kee R J, Miller J A and Jefferson T H 1980 A general-purpose, problem-independent, transportable, Fortran chemical kinetics code package *Sandia Report* SAND 80-8003